Control strategy design for forced fly-around of spacecraft against the tumbling target based on differential geometric principle

Yuan-he LIU, Yan-gang LIANG*, Jian-yong ZHOU, Jiu-tian LI

National University of Defense Technology, College of Aerospace Science and Technology, Hunan Changsha 410072, China

Abstract: Forced fly-around of spacecraft against the tumbling target is the basis for tracking and capturing a space tumbling target by a spacecraft. In this paper, the relative kinematic equations of the spacecraft and the target are first obtained with the help of the classical differential geometry theory. Considering the attitude kinematic of the tumbling target, the sliding model controller is designed to control relative motions along the line of sight (LOS) and perpendicular to LOS in the instantaneous rotating plane of the LOS. Finally, the effectiveness and robustness of the control strategy are verified by numerical simulation examples.

Key word: *space tumbling target, forced fly-around, attitude dynamics, sliding model control*

1. Introduction

With the continuous development of space industry, the amount of objects in space is more than 20,000. The deterioration trend of space environment becomes more obvious with the further increase of orbit spacecraft and debris. The Orbit Express Program of DAPRA is used to demonstrate the feasibility of rescue, maintenance, refueling and debris removal for on-orbit spacecraft. One of the key technologies is the automatic hovering, fly-around and capturing of on-orbit spacecraft [1] [2] [3] .

In the capture mission, the space target may exhibit a complex motion with spin and nutation. The spin axis may point in any direction. Before capturing a space tumbling target, it is necessary to complete the process of target detection, feature modeling, capture point selection and simultaneous approximation. One of the necessary ways for the capture mission is forced fly around the tumbling target [4].

*Corresponding author

E-mail: liangyg@nudt.edu.cn
Tel: +8613787014571

Sliding mode control (SMC), a mature robust control method, first appeared in the 1950s. It has been widely used in various engineering fields [5]. Essentially, SMC is a special kind of nonlinear control, whose nonlinearity is the discontinuity of control. Because the sliding surface can be designed and is irrelevant with the parameters and disturbances of controlled plant, SMC has the advantages of fast response, insensitivity to parameter changes and disturbances and simple physical implementation. In addition, there is no need for online identification when the control method is SMC.

Because the relative motion equations of the close-range spacecraft is nonlinear, the traditional linear control method cannot meet the requirements in practical case. As a result, a novel nonlinear control strategy needs to be explored.

This paper first explores the motion law of space curve based on classical differential geometry principle. Then the LOS rotation coordinate system and relative motion equations are constructed, which take the barycenter of spacecraft as the origin. The relative motion equations are decoupled into the instantaneous rotation plane of LOS (IRPL) and the rotation of IRPL. This paper considers the attitude motion of the tumbling target, controls the relative position of the spacecraft and the target to remain unchanged, realizes the synchronous flying around the tumbling target, and provides a stable operation platform for docking or catching subsequently [6] .

2. The attitude dynamic model of tumbling target

In order to achieve synchronous flying around the tumbling target, it is necessary to analyze the attitude motion of the target at first. Without losing generality, it can be assumed that the three axes of the principal axis coordinate system are respectively the principal axis of inertia and the origin is at the center of mass of the target. When the tumbling target is not affected by the external moment, the symmetrical axis of mass distribution is taken as z_I for the regular precession target, and the other two inertia principal axes are x_I and y_I respectively, which satisfy the right-hand rule. For the Euler-Poinsot case, the selected coordinate axes should satisfy the right-hand rule, and the corresponding rotational inertia of each axis satisfies $I_z < I_x < I_y$ or $I_z > I_x > I_y$.

The axis of the reference coordinate system is in the same direction with the angular momentum vector. Ox_r is on the intersection of the $Ox_r z_r$ plane and the plane at the initial time, and the angle between Ox_r and Ox_I is not obtuse. Oy_r is determined according to the right hand. The transformation relationship between the principal axis coordinate system and the reference coordinate system is shown in the following figure. The Euler angles are precession angle ϕ , nutation angle θ and spin angle φ respectively in the 313 rotation order.

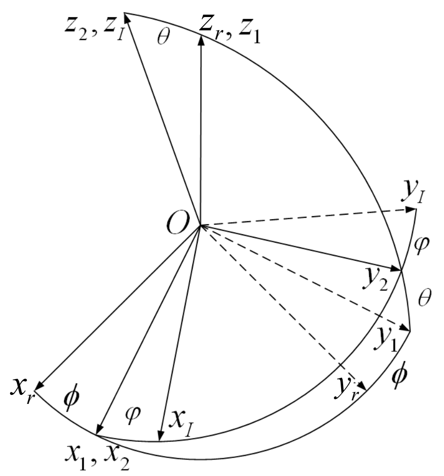

Fig.1 The geometry relationship between the Body frame and the Reference frame

When the tumbling target is not affected by the external moment, the dynamic equation of rotation around the center of mass is established in the principal axis coordinate system[7]:

$$\begin{cases} I_x\dot{\omega}_x-\left(I_y-I_z\right)\omega_y\omega_z=0 \\ I_y\dot{\omega}_y-\left(I_z-I_x\right)\omega_z\omega_x=0 \\ I_z\dot{\omega}_z-\left(I_x-I_y\right)\omega_x\omega_y=0 \end{cases} \tag{1}$$

where I_x, I_y and I_z are principal axes of inertia. ω_x, ω_y, and ω_z are the component of the rotational angular velocity vector $\boldsymbol{\omega}$ of the tumbling target in the reference coordinate system.

In the short period of capturing, the motion of the target satisfies the conservation laws of kinetic energy and angular momentum without considering the disturbance force and moment. According to the law of conservation of kinetic energy and angular momentum, $\boldsymbol{\omega}$ is projected into the principal axis coordinate system:

$$\begin{cases} \omega_x=\dot{\phi}\sin\theta\sin\varphi+\dot{\theta}\cos\varphi \\ \omega_y=\dot{\phi}\sin\theta\cos\varphi-\dot{\theta}\sin\varphi \\ \omega_z=\dot{\varphi}+\dot{\phi}\cos\theta \end{cases} \tag{2}$$

The angular momentum vector $\boldsymbol{H}=\boldsymbol{I\omega}$ is projected into the principal axis coordinate system:

$$\begin{cases} I_x\omega_x=H\sin\theta\sin\varphi \\ I_y\omega_y=H\sin\theta\cos\varphi \\ I_z\omega_z=H\cos\theta \end{cases} \tag{3}$$

By simplifying Eq. (2) into Eq. (3), it can be obtained that:

$$\begin{cases} \dot{\phi} = \omega_0 \left[\rho + (\lambda - \rho) \sin^2 \varphi \right] \\ \dot{\theta} = \omega_0 (\lambda - \rho) \sin\theta \cos\varphi \sin\varphi \\ \dot{\varphi} = \omega_0 \cos\theta \left[1 - \rho - (\lambda - \rho) \sin^2 \varphi \right] \end{cases} \tag{4}$$

where $\lambda = I_z / I_x$, $\rho = I_z / I_y$, $\omega_0 = H / I_z$. The Euler angle at any time can be calculated if it is known without external moment at $t = 0$.

When the motion of tumbling target is regular precession, it is assumed that the mass of the tumbling target is asymmetrically distributed with respect to *Oz*, namely $\lambda = \rho$.

When the tumbling target is in Euler-Poinsot motion, assuming $I_z < I_x < I_y$ or $I_z > I_x > I_y$, Euler-Poinsot motion requires an acute nutation angle

The parameters of the target's moment of inertia, initial angular momentum and initial Euler angle (313 rotation) are shown in Table 1.

The Euler angular rate curves of the target in regular precession motion and Euler-Poinsot motion are obtained by simulation, as shown in Figs. 2 and 3. Fig. 2 shows that the nutation angular rate of the regular precession target is zero, precession angular rate and spin angular rate are constant, and the target moves periodically with constant Euler angular velocity. Fig. 3 shows that the nutation angular rate of Euler-Poinsot motion target changes periodically near zero, and the precession angular rate and spin angular rate also change periodically, but their mean value is larger than that of nutation angular rate.

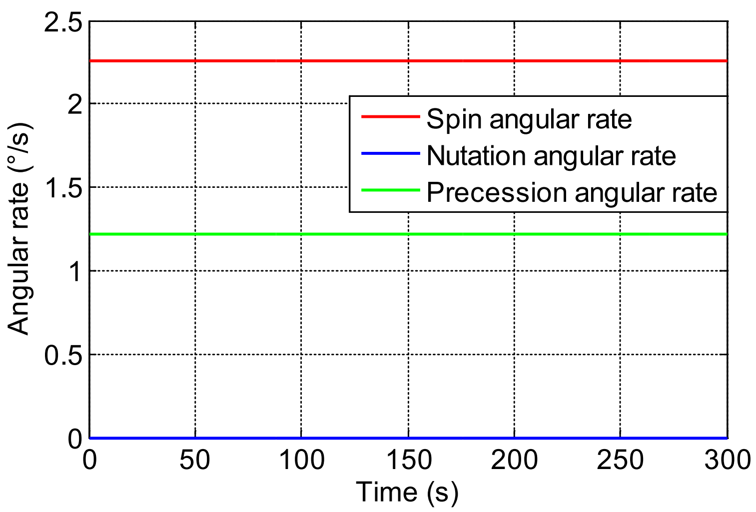

Fig.2 Eulerian angular rate of regular precession target

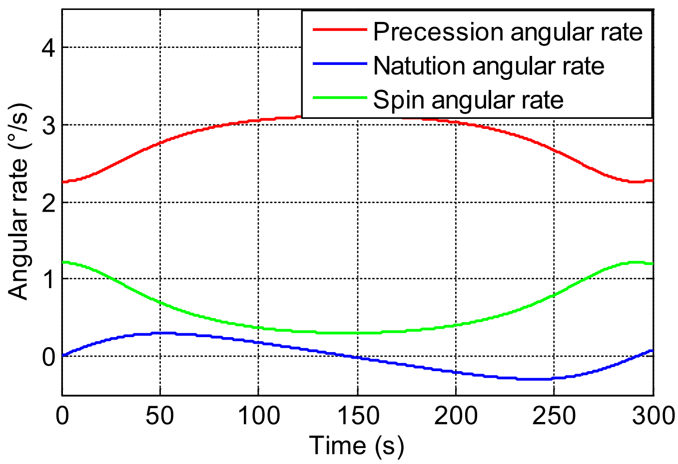

Fig.3 Eulerian angular rate of Euler-Poinsot target

Table.1 Rotational inertia, initial angular momentum and initial Euler angle parameters of target

Target	I_x(kg·m^2)	I_y(kg·m^2)	I_z(kg·m^2)	H(kg·m^2/s)	φ(°)	θ(°)	φ(°)
regular precession	8400	8400	5070	331.0627	65	35	0
Euler-Poinsot	8000	8400	5070	331.0627	65	35	0

3. Control strategy design

In order to reduce the dependence of control strategy design on measurement information and target estimation information and improve control robustness, Chiou and Kuo applied the classical differential geometry method to the geometric analysis of space interception[8][9]. The motion equation of space curve based on classical differential geometry is studied by Li et al [10][11]. The three-dimensional motion equation in line-of-sight rotating coordinate system:

$$\begin{cases} \dfrac{\mathrm{d}\boldsymbol{e}_r}{\mathrm{d}t} = \omega_s \boldsymbol{e}_\theta \\ \dfrac{\mathrm{d}\boldsymbol{e}_\theta}{\mathrm{d}t} = -\omega_s \boldsymbol{e}_r + \Omega_s \boldsymbol{e}_\omega \\ \dfrac{\mathrm{d}\boldsymbol{e}_\omega}{\mathrm{d}t} = -\Omega_s \boldsymbol{e}_\theta \end{cases} \tag{5}$$

where $\boldsymbol{e}_r$ of LOS rotation coordinate system is parallel to LOS, $\boldsymbol{e}_\omega$ is consistent with the direction of LOS rotation angular velocity, and $\boldsymbol{e}_\theta$ is determined by the right hand. $\boldsymbol{e}_r$ and $\boldsymbol{e}_\theta$ form the IRPL.

The relative motion equation in the LOS rotation coordinate system actually divides the rotation of LOS into two parts: the rotation of LOS in the instantaneous rotation plane and the rotation of the instantaneous rotation plane, which are represented by $\boldsymbol{\omega}_s$ and $\boldsymbol{\Omega}_s$ respectively. $\boldsymbol{\omega}_s$ is the LOS angular velocity, $\boldsymbol{\omega}_s = \omega_s \boldsymbol{e}_\omega$. $\boldsymbol{\Omega}_s$ is the angular velocity of IRPL, $\boldsymbol{\Omega}_s = \Omega_s \mathrm{e}_r$.

The relative motion equation in LOS rotation coordinate system is as follows:

$$\begin{cases} \ddot{r} - r\omega_s^2 = a_{tr} - a_{cr} \\ r\dot{\omega}_s + 2\dot{r}\omega_s = a_{t\theta} - a_{c\theta} \\ r\omega_s \Omega_s = a_{t\omega} - a_{c\omega} \end{cases} \tag{6}$$

where a_t and a_c represent the acceleration of the target and spacecraft respectively, and the subscripts " r , θ and ω " represent the components of the control acceleration along three axes respectively. The first two formulas represent the changes of the LOS rotation rate and the relative distance between the spacecraft and the target in IRPL, and the third one represents the rotation of IRPL. The first two formulas are decoupled from the third, which reduces the complexity of the problem.

The control strategy design of forced fly-around requires controlling the rotation of IRPL to coincide with the fly-around plane, and then constructing the control law of fly-around in IRPL. The control force along $\boldsymbol{e}_\omega$ can control IRPL, and the control acceleration can be calculated from the control acceleration in $\boldsymbol{e}_r$ and $\boldsymbol{e}_\theta$.

There are uncertainties and errors in the measurement and control of space tumbling targets. For example, there is residual thrust on the tumbling target in some cases, and there is error in the actual control force of the spacecraft. Therefore, the uncertainty of measurement and control deviation must be taken into account in the process of fly-around. Eq. (6) can be transformed into:

$$\begin{cases} \ddot{r} - r\omega_s^2 = w_r(t) - a_{cr} \\ r\dot{\omega}_s + 2\dot{r}\omega_s = w_\theta(t) - a_{c\theta} \\ r\omega_s \Omega_s = 0 \end{cases} \tag{7}$$

where $w_r(t)$ and $w_\theta(t)$ are the errors of $\boldsymbol{e}_r$ and $\boldsymbol{e}_\theta$ in IRPL, and the upper bounds are d_r and d_θ :

$$|w_r(t)| \le d_r, \quad |w_\theta(t)| \le d_\theta \tag{8}$$

The control strategy consists of two steps:

(1) Control the flying radius of the spacecraft: keep the relative distance along LOS unchanged.

A SMC strategy based on exponential reaching law is designed to control t the relative distance along LOS. The first formula of Eq. (7) can be transformed into:

$$\ddot{r} = r\omega_s^2 + u + w_r(t) \tag{9}$$

where r is the relative distance, $\ddot{r}$ is the relative acceleration, and u is the control acceleration in the line of sight direction.

Defining relative distance error:

$$e = r - r_d \tag{10}$$

where r_d is the expected flying radius. Then the axial speed error and acceleration error are:

$$\begin{cases} \dot{e} = \dot{r} - \dot{r}_d \\ \ddot{e} = \ddot{r} - \ddot{r}_d \end{cases} \tag{11}$$

where $\dot{r}_d$ is the expecting approaching speed along LOS, $\ddot{r}_d$ is the expecting approaching acceleration, $\dot{r}_d = 0, \ddot{r}_d = 0$.

Sliding mode function is designed as：

$$s(t) = ce(t) + \dot{e}(t) \tag{12}$$

where c satisfies Hurwitz polynomial condition. As a result, we get

$$\begin{aligned} \dot{s}(t) &= c\dot{e}(t) + \ddot{e}(t) = c(\dot{r} - \dot{r}_d) + (\ddot{r} - \ddot{r}_d) \\ &= c\dot{r} + r\omega_s^2 + u(t) + w_r(t) \end{aligned} \tag{13}$$

The exponential reaching law is adopted:

$$\dot{s} = -\varepsilon \operatorname{sgn} s - ks, \varepsilon > 0, k > 0 \tag{14}$$

The sliding mode control law is obtained by combining the upper equation:

$$u(t) = -c\dot{r} - r\omega_s^2 - \varepsilon \operatorname{sgn} s - ks - w_r(t) \tag{15}$$

where c, k, ε are the control parameters, the larger k is, the faster the approaching speed is; the smaller ε is, the smaller the chattering is.

Obviously, the above control law cannot be realized due to the unknown disturbance $w_r(t)$,. In order to solve this problem, the control law is designed by using the boundness of disturbance. The disturbance $w_r(t)$ in equation (15) is replaced by a positive real number d_c , which is brought into equation (13) to obtain:

$$\dot{s} = -\varepsilon \operatorname{sgn} s - ks + d_c - w_r(t) \tag{16}$$

In order to guarantee that $s(t)$ and $\dot{s}(t)$ are not aliased, let $d_c = d_r \operatorname{sgn}(s)$.

Finally, the following SMC law is obtained:

$$u(t) = -c\dot{r} - r\omega_s^{\,2} - \varepsilon \operatorname{sgn} s - ks - d_c \tag{17}$$

In order to prove the asymptotic stability of the control rate, the Lyapunov function $V = 1/2s^2$ is defined, and the derivatives (9) and (17) are introduced, we get

$$\begin{aligned} \dot{V} &= s\dot{s} = s(c\dot{e} + \ddot{e}) = s\left[c\dot{r} + r\omega_s^{\,2} + u(t)\right] \\ &= s\left[c\dot{r} + r\omega_s^{\,2} + \left(-c\dot{r} - r\omega_s^{\,2} - \varepsilon \operatorname{sgn} s - ks\right)\right] \\ &= -s(\varepsilon \operatorname{sgn} s + ks) = -\varepsilon|s| - ks^2 < 0 \end{aligned} \tag{18}$$

According to Lyapunov stability theory, the closed-loop system is globally asymptotically stable.

(2) Control the forced fly-around rate of the spacecraft: keep the LOS rotation rate is consistent with the target spin rate.

A SMC strategy based on exponential reaching law is designed to control LOS rotation rate too. The second formula of Eq. (7) can be transformed into:

$$r\dot{\omega}_s = -2\dot{r}\omega_s + w_\theta(t) + u(t) \tag{19}$$

The sliding surface design is as follows:

$$s = r_d\dot{\varphi}_d - r\omega_s \tag{20}$$

So we can get

$$\begin{aligned} \dot{s} &= \dot{r}_d\dot{\varphi}_d + r_d\ddot{\varphi}_d - \dot{r}\omega_s - r\dot{\omega}_s \\ &= \dot{r}\omega_s - w_\theta(t) - u(t) \end{aligned} \tag{21}$$

The exponential reaching law is adopted:

$$\dot{s} = -\varepsilon \operatorname{sgn} s - ks, \varepsilon > 0, k > 0 \tag{22}$$

The SMC law is obtained by combining the upper formula and considering the boundness of the disturbance.

$$u(t) = \varepsilon \operatorname{sgn} s + ks + \dot{r}\omega_s - d_c \tag{23}$$

In order to guarantee that $s(t)$ and $\dot{s}(t)$ are not aliased, let $d_c = d_\theta \operatorname{sgn}(s)$.

According to Lyapunov stability theory, the closed-loop system is globally asymptotically stable. The process is similar to the controller design along LOS.

In engineering practice, the thrust of the engine is limited, so the control input saturation function is introduced:

$$sat(u) = \begin{cases} u, & |u| < A_{sat} \\ A_{sat} \operatorname{sgn}(u), & |u| > A_{sat} \end{cases} \tag{24}$$

where A_{sat} is the maximum acceleration limit of the spacecraft, and $\operatorname{sgn}(\cdot)$ is a symbolic function.

4. Numerical simulation

In this section, numerical simulation is used to verify the effectiveness of the designed control strategy. The simulation scenario is set as relative motion control in ultra-close range. Considering the attitude motion of the target, the forced flight of the spacecraft around the tumbling target is shown in Fig. 4. The fly-around plane and the spinning plane coincide, that is, IRPL is perpendicular to the spin axis of the tumbling target. In this case, the speed of synchronous fly-around is equal to the target spin rate, and the radius of flying around remains unchanged. This kind of flying around can achieve stable hovering of LOS at any position of the target in the rotation plane.

4.1 Forced fly-around for regular precession target

SMC is used to control both the direction along LOS and perpendicular to LOS. The control parameters along LOS are selected as follows: $c=[0.01,0.001]$, $k=0.05$, $\varepsilon=0.001$. The control parameters perpendicular to LOS are selectied as follows: $k=0.1$, $\varepsilon=0.5$. The upper limit of control acceleration saturation function is $A_{sat}=1$. The simulation step size is set to 0.1s. The simulation time is 300s. As shown in Fig. 2, the spin rate of the regular precession target is 2.25°/s。Assuming that the target maneuvering acceleration is: $\boldsymbol{a}_t=0.01\boldsymbol{x}_s+0.01\boldsymbol{y}_s+0.01\boldsymbol{z}_s$, and controlling deviation can be set to $w_r(t)=w_\theta(t)=0.01$.

The initial orbital elements of the target and spacecraft are shown in Table 2. The simulation results are shown in Fig. 5-8.

Table.2 Initial orbital elements of target and spacecraft

Orbital elements	a(km)	e	i(°)	Ω(°)	ω(°)	f(°)
Target	7158.14	0.01	30	120	60	30
Spacecraft	7158.34	0.01	30	120	60	30

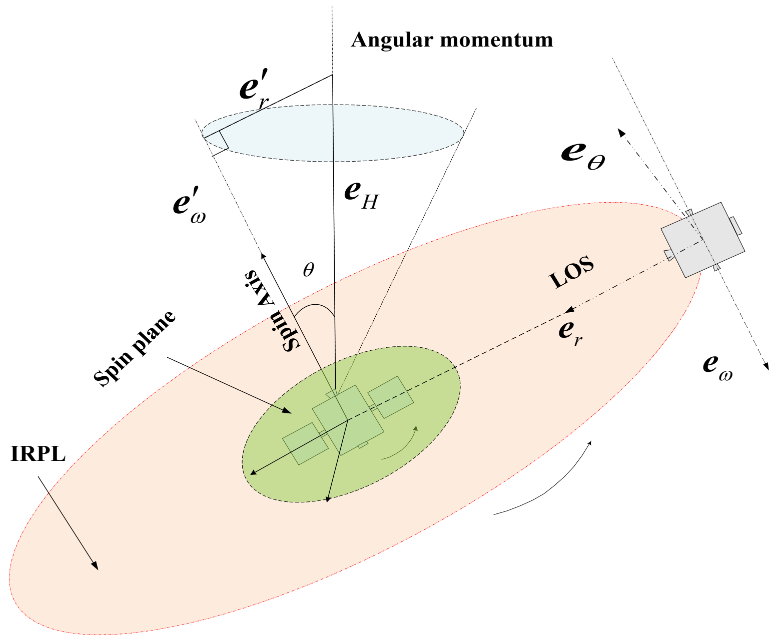

Fig.4 Forced fly-around schematic

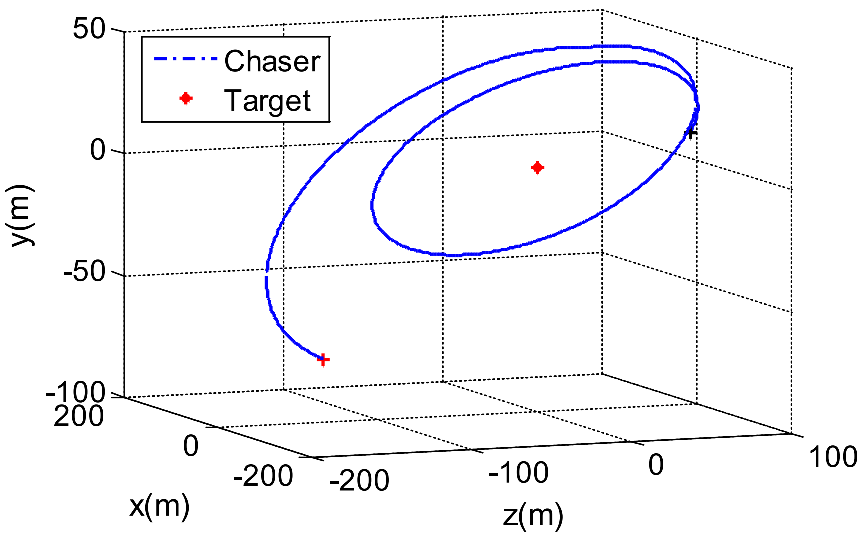

Fig.5 The relative motion trajectory of target and spacecraft

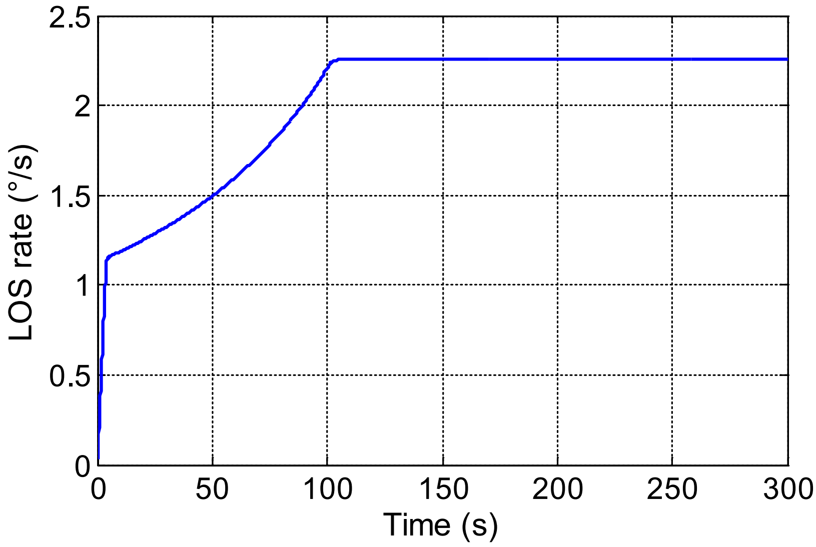

Fig.6 The curve of line of sight

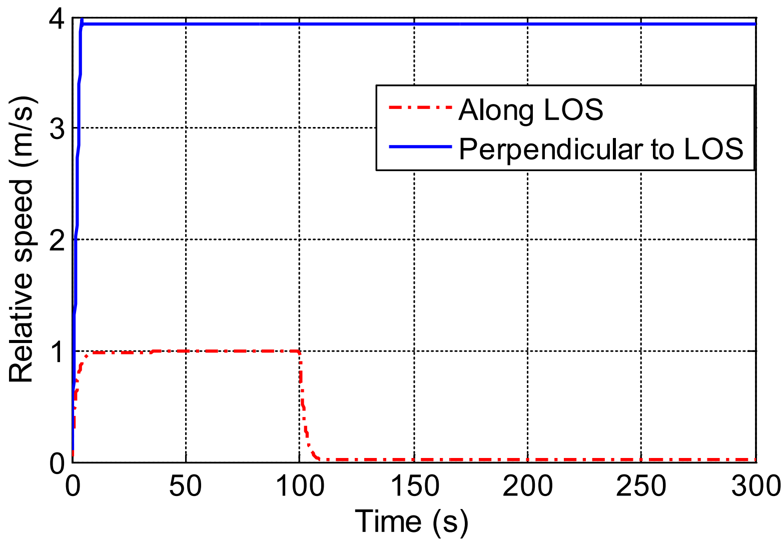

Fig.7 The curve of relative velocity

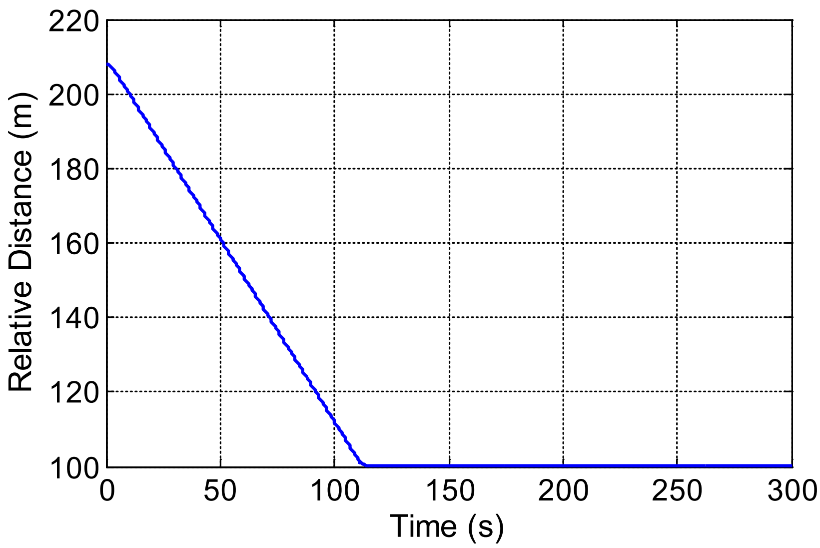

Fig.8 The curve of relative distance

The spacecraft first maneuvers to the spin plane of the target, and then makes a steady forced fly-around after 100s. From Fig. 5, it can be seen that the flight circle is about one and a half in 300s. In Fig. 6, the LOS rotation increases gradually, and finally stabilizes near the spin angular rate, which proves the effectiveness of the control law perpendicular to LOS. In Fig. 7, the approaching speed along LOS is about 1m/s before 100s, and then decreases to 0. The relative speed perpendicular to LOS increases first, and then stabilizes near 4m/s. In Figure 8, the spacecraft approaches the target first, and the relative distance between the spacecraft and the target stabilizes at 100 meters after 110s, with an error of less than 0.1%. The speed increment of the spacecraft is about 24.7m/s per circle.

4.2 Forced fly-around for Euler-Poinsot target

The control parameter settings are the same as those in section 4.1. The simulation results are shown in Figs. 9-12.

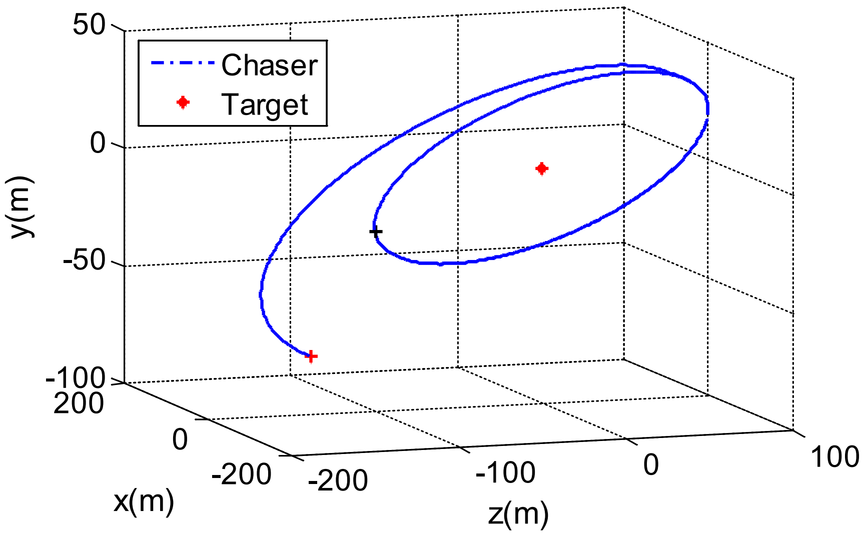

Fig.9 The relative motion trajectory of target and spacecraft

The spacecraft first maneuvers to the spin plane of the target, and then makes a steady forced flight around the target after 100s. From Fig. 9, it can be seen that there are about two circles in 300s. In Fig. 10, the LOS rotation increases first and then stabilizes around the target spin rate. Fig. 11 shows that the relative speed along LOS first increases to about 1m/s, then decreases to 0 after 100s. It shows that the spacecraft approaches the target along the line of sight first, then stabilizes around. In addition, the relative speed perpendicular to LOS increases rapidly, then changes slowly around the target spin rate. In Figure 12, the relative distance between the spacecraft and the target decreases first, and finally stabilizes at 100 meters, with an error of less than 0.1%. The speed increment of the spacecraft is about 30.2m/s per circle.

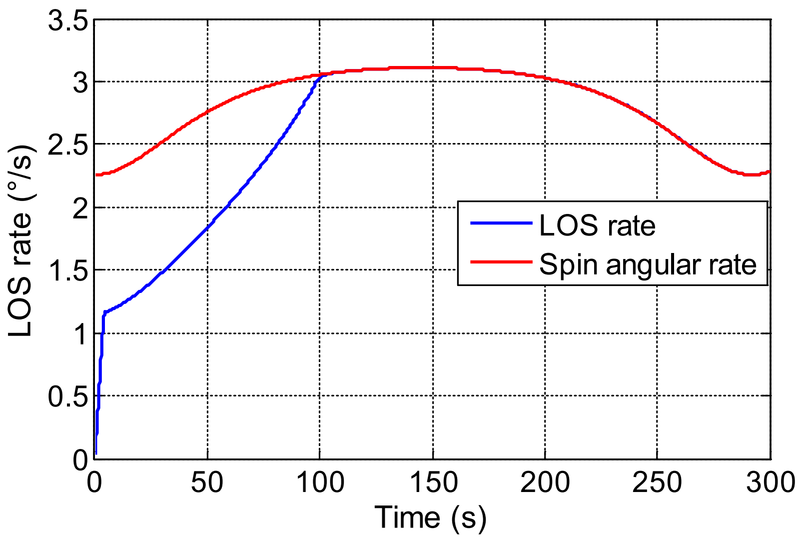

Fig.10 The curve of line of sight

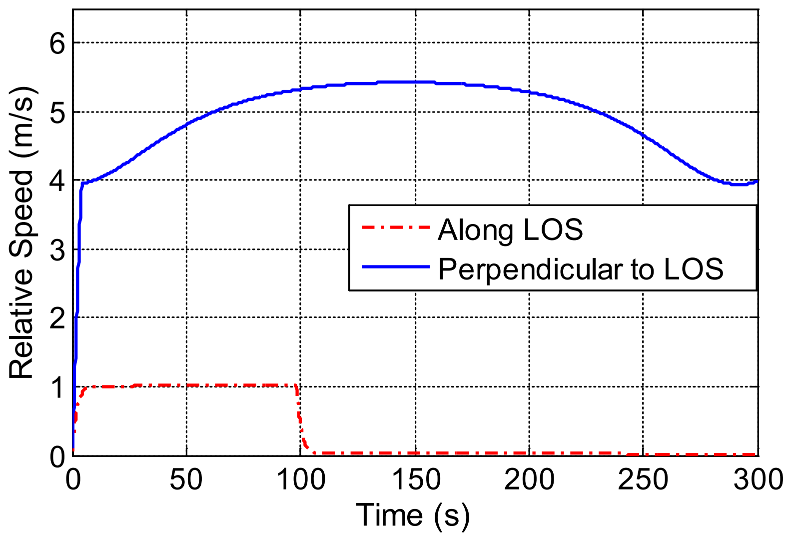

Fig.11 The curve of relative velocity

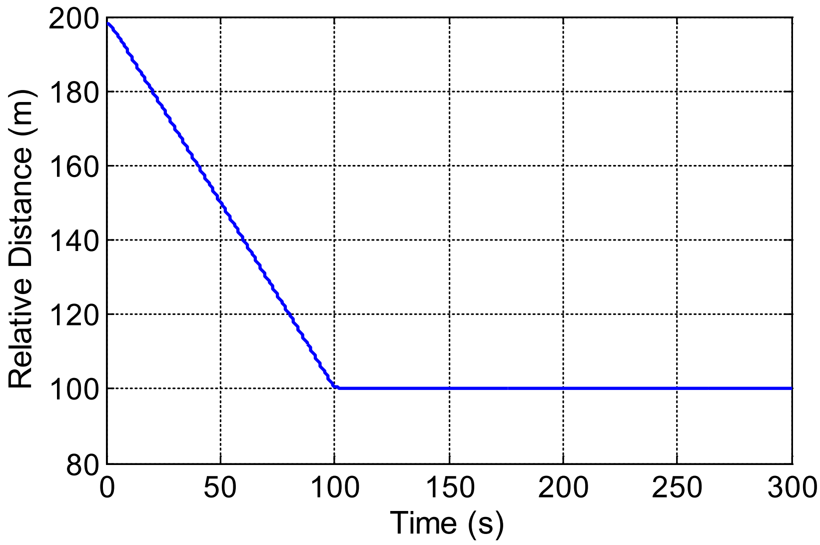

Fig.12 The curve of relative distance

5. Conclusions

In this paper, a control strategy of forced fly-around of spacecraft against the tumbling target based on classical differential geometry is proposed for the first time. The attitude motion of the space tumbling target is described by Euler angle. The relative motion equation is established in the instantaneous rotation coordinate system. The three-dimensional problem are transformed into two-dimensional problem as the motion decouples whose physical meaning is clear. Considering measurement uncertainties and control errors, SMC based on exponential reaching law is adopted in tIRPL along and perpendicular to LOS. The simulation results show that the method has good control performance and robustness, and can realize synchronous fly-around of spacecraft against the tumbling target.

Acknowledge

This work was supported by the Major Program of National Natural Science Foundation of China under Grant Numbers 61690210 and 61690213. The authors would like to thank the anonymous reviewers for their helpful comments.

Reference：

[1] Matsumoto S, Dubowsky S, Jacobsen S, et al. Fly-by approach and guidance for uncontrolled rotating satellite capture[C]. AIAA Guidance, Navigation, and Control Conference and Exhibit. 2003: 5745.

[2] Arantes G, Martins-Filho L S. Guidance and control of position and attitude for rendezvous and dock/berthing with a noncooperative target spacecraft[J]. Mathematical Problems in Engineering, 2014, 2014.

[3] Sidi M J. Spacecraft dynamics and control: a practical engineering approach[J]. Contemporary Physics, 1997, 10(6):118.

[4] Wang Weilin. Mission plan of active debris r 1emoval and design of guidance and control techniques applying space maneuver vehicle[Doctoral Dissertation] [D].Graduate School of National University of Defense Technology, Changsha, Hunan, China. April 2017.

[5] Liu Jinkun. Sliding mode control design and MATLAB simulation(Third Edition): the basic theory and design method[M]. Beijing: Tsinghua University Press. 2015.

[6] Weilin Wang, Kebo Li, Lei Chen, Yongjun Lei. Guidance law design for forced fly-around[C]. 3rd IAA Conference on Dynamics and Control of Space Systems, Russia, 2017

[7] Huang Zhengui. Spacecraft attitude dynamics[M]. Changsha: National University of Defense Technology Press. 1997.

[8] Chiou Y C, Kuo C Y. Geometric Approach to Three Dimensional Missile Guidance Problems [J]. Journal of Guidance, Control, and Dynamics, 1998, 21(2): 335–341.

[9] Chiou Y C, Kuo C Y. Geometric Analysis of Missile Guidance Command [J]. IEEE Proceedings: Control Theory and Applications, 2000, 147(2): 205–211.

[10] Li Kebo. Differential geometry guidance law for intercepting maneuvering target [Master Dissertation] [D]. Graduate School of National University of Defense Technology, Changsha, Hunan, China. November 2010.

[11] Chen L, Li K, Liang Y. Dimension-reduction method of three-dimensional guidance laws[C]. AIAA Guidance, Navigation, and Control Conference. 2012: 4688.